

Single-End Fault Location Algorithm for Series-Compensated Parallel Transmission Lines Using Only Current Measurement

Mohsen Ansari

Department of Electrical Engineering, University of Guilan, Iran

Abstract: The environmental concerns, limitation of building new transmission lines, increasing transmittable power and reducing transmission losses are among the main reasons to install series capacitors on transmission lines. In this paper, the authors have proposed a new algorithm which utilizes the positive sequence network, in order to determine the fault location on series compensated parallel transmission lines. The proposed scheme is based on the superposition positive sequence current signal from local end. The proposed method does not require voltage signals as well as remote-end data. Furthermore, it eliminates effects of series compensation and mutual coupling on locating fault point. To evaluate the proposed method, different fault scenarios were simulated on 400kV, 300km series compensated parallel transmission line using EMTDC/PSCAD software. The result of simulations determines the high accuracy of the proposed method in pinpointing faults.

Keywords: Fault location, local measurement, parallel line, power system faults, series capacitor.

I. INTRODUCTION

Nowadays, transmission lines are operating closer to their margins to provide electricity to the increasing demand of utilities. Several methods have been proposed to increase the capability of transferring power on existing due to new right of ways restriction, cost and environmental aspects. Parallel transmission lines, series compensated transmission lines and combinations of these two methods are the most significant ways which can be applied to increase the power transfer rate.

Transmission lines experience faults due to various reasons such as extreme weather condition, vegetation growing, animals and human failures. Since, the transmission lines are spread across hundreds of miles, it is necessary to utilize a fault location method which can determine the location of a fault accurately. Therefore, maintenance crews can restore the power system to its normal operating conditions within proper time.

Different fault location algorithms were proposed in literatures [1-20]. Single-end impedance based fault location methods are considered the most conventional scheme [1-9]. The main feature of these methods is the low cost of implementation. However, these methods could be affected by infeed current, fault resistance or fault incidence angle.

Several methods were developed using unsynchronized two-end measurements [10-17]. The main feature of such methods comparing to single-end ones is the higher accuracy. However, availability of measurements through the entire power system might not be accessible due to the cost and installation concerns.

Several researchers developed methods to locate faults in double circuit transmission lines [18-24]. However, the accuracy of single-end methods is less; they rely only on measurements captured at local end. Therefore, they don't need communication links which results in cheaper implementation in the network.

So far, different methods were developed to locate faults in series-compensated lines [25-30]. In [28], artificial neural network along with impedance based method is used to locate faults. In [29], the proposed algorithm determines the location of fault in both uncompensated and series-compensated parallel transmission line. In [30], different traveling

wave methods were considered to locate faults on teed lines with various possible line configurations considering parallel circuits and series compensation.

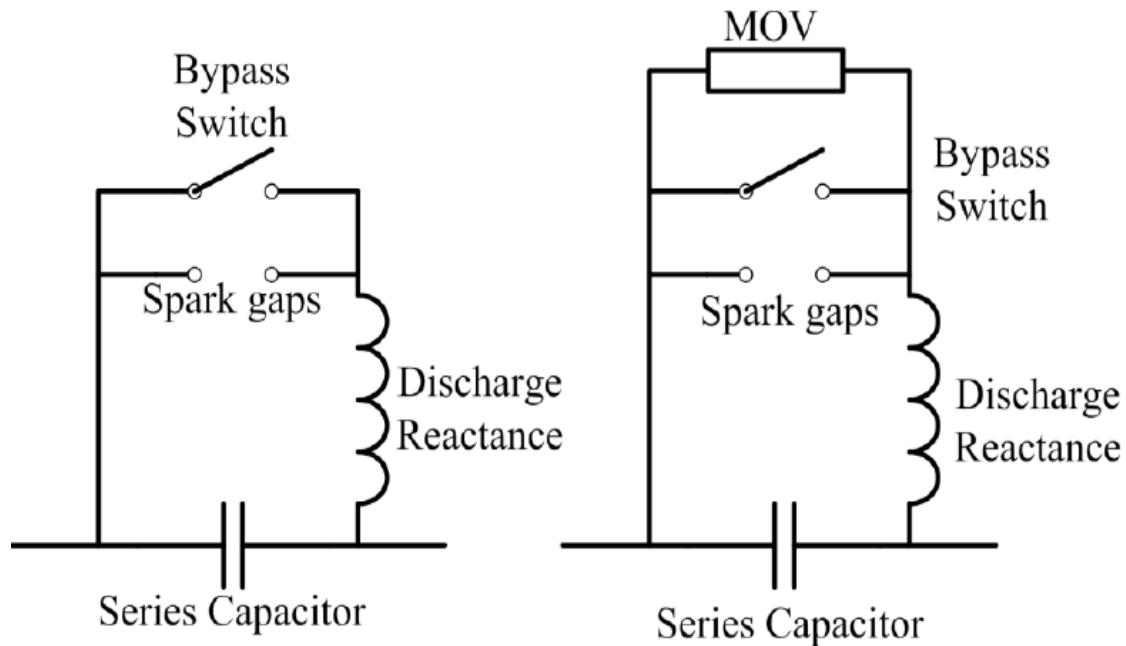


Fig. 1. Two typical Protection scheme for SCs

In this paper, a novel technique is proposed to locate faults on series-compensated parallel transmission lines. The proposed method is using positive sequence components of currents measured at the local end. First, the algorithm is obtained considering series compensated capacitor banks installed at two ends of transmission lines. Then, it is expanded to be applicable for series compensation in the middle of transmission lines. The proposed algorithm calculates the location of fault irrespective of variations of different fault parameters, such as series compensation level, fault distance, fault inception angle and fault resistance. The assumption is that transmission lines are fully transposed which allows utilization of symmetrical components theory.

II. BACKGROUND THEORY

A. Series Capacitor Protection:

Series capacitors (SCs) must be protected through Metal Oxide Varistors (MOVs) to minimize the damage caused by over-voltages across SCs (Fig.1). If the voltage across SC exceeds a given value, gap or MOV flash over to avoid extra voltage on SC terminals. However, if the fault current is low, they may not be triggered. Hence, in such cases, the SC acts as a pure reactance.

If the fault current is high enough, the voltage drop across the SC would be far above the protection level of MOV, causing all the current passes through MOVs. Consequently, in such cases, the SC acts as a small resistance equal to MOV resistance characteristic.

Between these two extreme boundaries, in several conditions, a comparable portion of current passes through each SC and MOV. Fig. 2 shows the situation where MOV clamp the voltage at certain level results in nonlinear equivalent impedance. In this example, the MOV is designed to clamp the voltage at 150 kV. The MOV operation does not fully remove the SC, however, it bypasses the SC when the MOV energy level go beyond a threshold.

If the fault current is higher, the voltage drop across the SC (Fig. 2.a) is closer rectangular shape. In each cycle, the SC passes the fault current during initial half-cycles (Fig.2.b) till the voltage across SC exceeds the threshold value. Then, the MOV conducts current during the remaining time to maintain the voltage level across the SC under the threshold value (Fig.2.c).

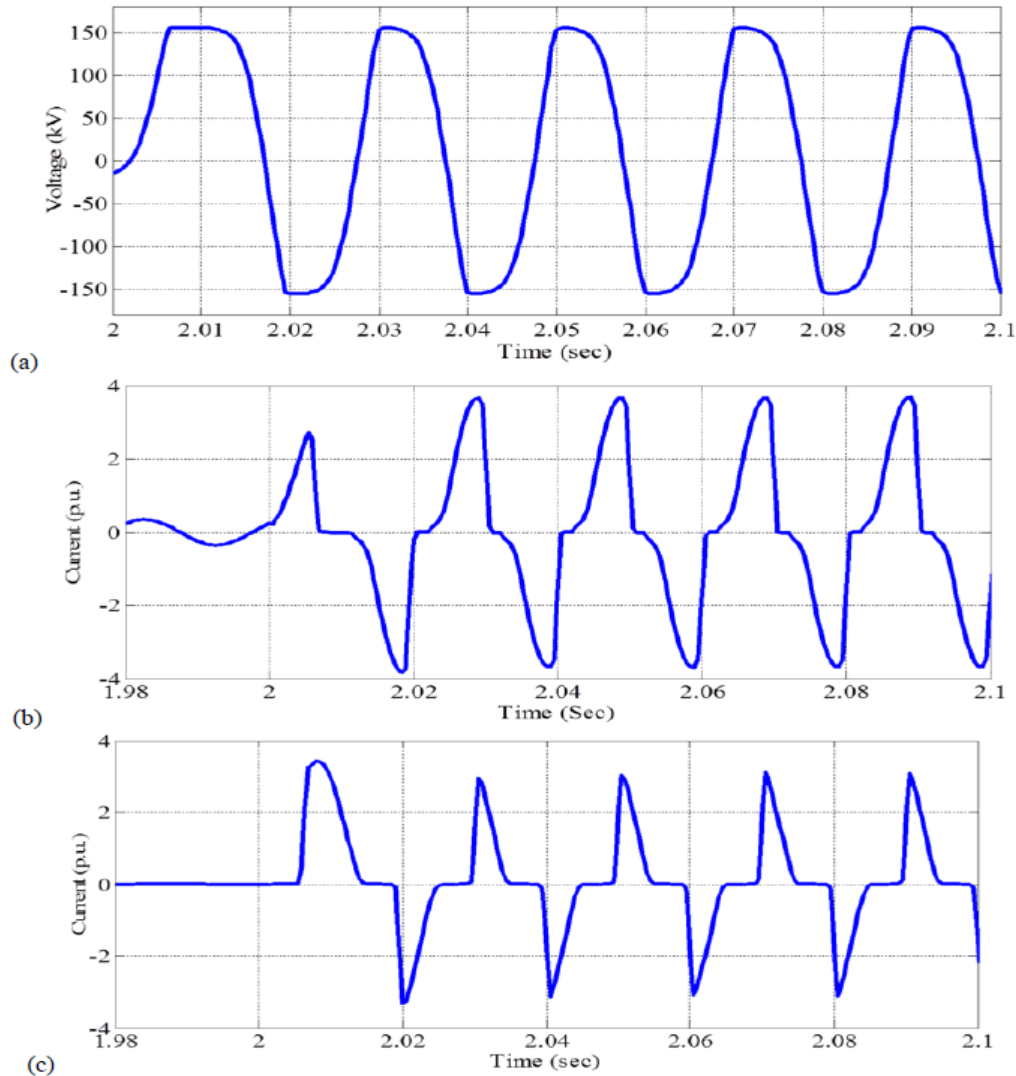


Fig. 2. (a) Voltage drop across the SC, (b) Current passes through capacitor, (c) Current passes through MOV

B. Series Capacitor & MOV Modeling:

To obtain an approximated equivalent impedance for SC protected by MOV as shown in Fig. 3.a, first we need to obtain a characteristic for voltage-current of MOV. In this fashion, (1) has been introduced and used in previous research studies [31]:

$$\frac{i_{MOV}}{p} = \left(\frac{V_{MOV}}{V_{ref}}\right)^q \quad (1)$$

where , q and V_{ref} are defined to calculate the knee-point as shown in Fig. 4 (In this case, MOV is designed to clamp the SC voltage at 200 kV).

Knowing (1), an MOV-protected SC can be approximated by equivalent series impedance (Fig. 3.b):

$$Z_{eq}(I_{pr}) = R_{eq}(I_{pr}) - jX_{eq}(I_{pr}) \quad (2)$$

The following model was proposed by Goldsworthy [31]:

$$R_{eq} = 0 \quad I_L < 0.98I_{pu} \quad (3)$$

$$X_{eq} = X_{SC} \quad I_L < 0.98I_{pu} \quad (4)$$

$$R_{eq} = X_{SC} \cdot (0.0745 + 0.49e^{-0.243I_{pr}} - 0.6e^{-1.4I_{pr}} - 35e^{-5I_{pr}}) \quad I_L > 0.98I_{pu} \quad (5)$$

$$X_{eq} = X_{SC} \cdot (0.101 + 0.005749I_{pr} + 2.088e^{-0.8566I_{pr}}) \quad I_L > 0.98I_{pu} \quad (6)$$

$$I_{pr} = \frac{I_L}{I_{pu}} \quad (7)$$

where X_{SC} is the nominal capacitor bank reactance and I_{pr} , is the normalized compensator current I_L based on the capacitor protective level current I_{pu} . Typical range for I_{pu} is 1 to 6 kA rms. (2) to (7) can be used to calculate the equivalent resistance and reactance of MOV-protected SC under normal or fault conditions.

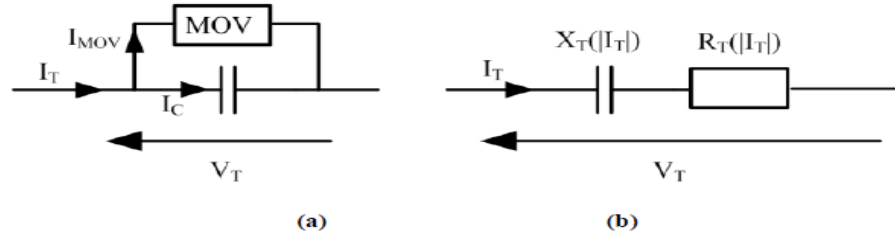


Fig. 3. (a) SC with MOV, (b) Equivalent impedance model

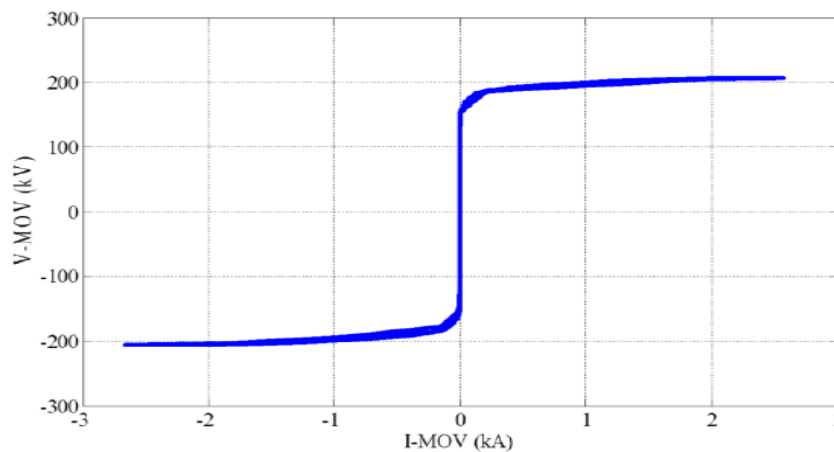


Fig. 4. Sample MOV Characteristic.

For instance, Figs. 5.a and 5.b show the equivalent resistance and reactance of MOV-protected SC, respectively. As the current passes through the MOV-protected SC increases, the absolute value of equivalent reactance decreases which indicates that the SC is bypassed by the MOV.

Although, the Goldsworthy's model of MOV-protected SC is useful in understanding of the phenomena, it is quite impractical to be used in modeling due to adding unnecessary calculation burden of solving nonlinear equations ((4) and (5)). On the other hand, many of power system applications such as fault location were defined based on symmetrical components which Goldsworthy's model cannot be applied on those applications. Next, a practical approach for symmetrical components will be introduced.

Considering the three phase SC, the following is three phase equivalent impedance of applies for the banks of three SCs and MOVs:

$$\begin{bmatrix} V_A \\ V_B \\ V_C \end{bmatrix} = \begin{bmatrix} Z_A & 0 & 0 \\ 0 & Z_B & 0 \\ 0 & 0 & Z_C \end{bmatrix} \cdot \begin{bmatrix} I_A \\ I_B \\ I_C \end{bmatrix} \quad (8)$$

where Z_A , Z_B and Z_C are Goldsworthy's equivalents of MOV-protected SC of phases A, B and C. Considering symmetrical component theory, Z_{012} impedance matrix can be calculated from (9).

$$Z_{012} = \frac{1}{3} \begin{bmatrix} Z_A + Z_B + Z_C & Z_A + a^2 \cdot Z_B + a \cdot Z_C & Z_A + a \cdot Z_B + a^2 \cdot Z_C \\ Z_A + a \cdot Z_B + a^2 \cdot Z_C & Z_A + Z_B + Z_C & Z_A + a^2 \cdot Z_B + a \cdot Z_C \\ Z_A + a^2 \cdot Z_B + a \cdot Z_C & Z_A + a \cdot Z_B + a^2 \cdot Z_C & Z_A + Z_B + Z_C \end{bmatrix} \quad (9)$$

Where a is a 120° shift operator.

Since, the three impedances (Z_A , Z_B and Z_C) might have different values, off diagonal elements in (9) could have different values. It can interpret that the sequence networks of MOV-protected SC is mutually coupled.

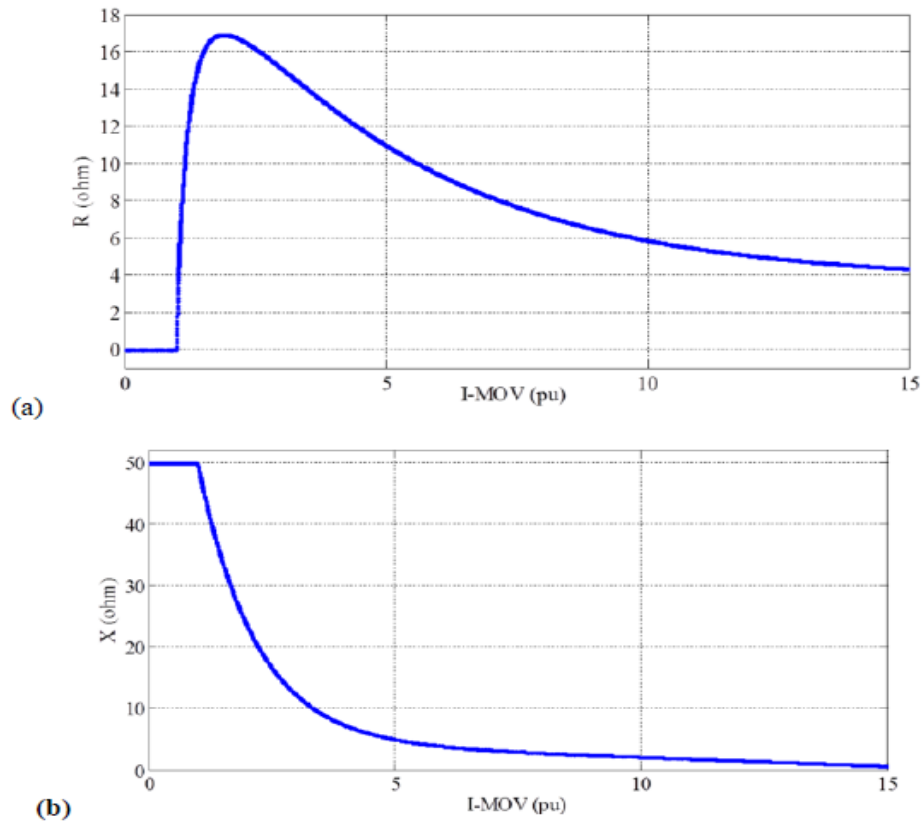


Fig. 5. (a) Equivalent resistance, (b) Equivalent reactance of MOV-protected SC vs. current

To address the problem, different conditions should be considered. In the case of high impedance faults (low fault current) or normal condition no current passes through MOVs.

$$Z_A = Z_B = Z_C = -jX_{SC} \quad (10)$$

Using (10), Z_{012} can be calculated as below:

$$Z_{012} = \begin{bmatrix} -jX_{SC} & 0 & 0 \\ 0 & -jX_{SC} & 0 \\ 0 & 0 & -jX_{SC} \end{bmatrix} \quad (11)$$

Hence, there is no mutual coupling between sequence networks under this conditions.

In second case, high current single phase fault is considered (for example a-g fault):

$$Z_A = 0, \quad Z_B = Z_C = -jX_{SC} \quad (12)$$

Using (12), Z_{012} can be calculated as below:

$$Z_{012} = \frac{1}{3} \cdot \begin{bmatrix} -2jX_{SC} & jX_{SC} & jX_{SC} \\ jX_{SC} & -2jX_{SC} & jX_{SC} \\ jX_{SC} & jX_{SC} & -2jX_{SC} \end{bmatrix} \quad (13)$$

In third case, high current double phase fault is considered (for example a-b fault):

$$Z_A = Z_B = 0, \quad Z_C = -jX_{SC} \quad (14)$$

Using (14), Z_{012} can be calculated as below:

$$Z_{012} = \frac{1}{3} \cdot \begin{bmatrix} -jX_{SC} & -jX_{SC} & -jX_{SC} \\ -jX_{SC} & -jX_{SC} & -jX_{SC} \\ -jX_{SC} & -jX_{SC} & -jX_{SC} \end{bmatrix} \quad (15)$$

Equations (13) and (15) show that the sequence network impedance matrices are mutually coupled. The complexity of mutually coupled sequence network can be addressed as follow.

For high current single phase fault, the voltage drop across faulty phase is negligible. In addition, voltage drop across healthy phases is small compared to faulty phase. Therefore, the mutual coupling of the sequence networks can be ignored.

For double phase faults, we can assume that the fault resistance is not high. Therefore, the SC will be bypassed in faulty phases which means that the voltage drop across faulty phases is negligible. On the other hand, due to small current in healthy phase, voltage drop across healthy phase is also negligible compare to faulty phases. Consequently, the mutual coupling of the sequence networks can be ignored.

Finally, it can be concluded that under proper assumptions, the symmetrical networks of MOV-protected SC is always decoupled.

III. PROPOSED FAULT LOCATION ALGORITHM

In this section the proposed single-end algorithm which utilizes only the current signals of parallel TL and the network impedance values will be introduced. The algorithm will be obtained for two types of series compensation. At first, the algorithm determines the location of fault for TL with series compensation at the two ends. Then the algorithm will be expanded to series compensation on the middle of TL.

A. Compensation at the Two Ends of TL:

Fig.6a illustrates the positive sequence network of a typical series compensated parallel TL which SC are located at two ends of TL in which an arbitrary fault happened at F_1 between Bus A and B. It is assumed that the fault locator under study is installed at bus A which calculates the fault distance using only current signals measured at the local bus A.

Fig.6b shows the same positive network before happening of the fault. In this figure the superposition pri stands for pre-fault condition.

Considering Figs. 6.a and 6.b and the superposition principle, one can conclude that the superposition of the positive sequence network would be same as Fig. 6.c, where $\Delta I_{A1} = I_{A1} - I_{A1}^{pri}$ and $\Delta I_{B1} = I_{B1} - I_{B1}^{pri}$ are the superposition positive current measured at Bus A.

Referring to Fig. 6.c, for a fault occurring at an arbitrary distance d_1 from Bus A, by applying KVL in loop which includes the Line B, (16) obtained as below:

$$[2 \cdot Z_{SC} + Z_{LB1}] \cdot \Delta I_{B1} + [(1 - d_1) \cdot Z_{LA1} + Z_{SC}] \cdot (I_{F1} - \Delta I_{A1}) - [d_1 \cdot Z_{LA1} + Z_{SC}] \cdot \Delta I_{A1} = 0 \quad (16)$$

Like (16), Referring to Fig. 6.c, for a fault occurring at an arbitrary distance d_1 from Bus A, by applying KVL in loop which includes the Line A, equation (17) obtained as below:

$$Z_{SA1} \cdot (\Delta I_{A1} + \Delta I_{B1}) + [2 \cdot Z_{SC} + Z_{LB1}] \cdot \Delta I_{B1} + Z_{SB1} \cdot (\Delta I_{A1} + \Delta I_{B1} - I_{F1}) = 0 \quad (17)$$

Elimination of I_{F1} from (16) and (17) yields the following formula for a sought distance to fault:

$$d_1 = \frac{Z_{SA1} + Z_{SC}}{Z_{LA1}} - \frac{Z_{SB1} \cdot (Z_{LA1} + 2 \cdot Z_{SC}) \cdot (\Delta I_{A1} + \Delta I_{B1})}{Z_{LA1} \cdot [(Z_{SA1} + Z_{SB1}) \cdot (\Delta I_{A1} + \Delta I_{B1}) + (Z_{LB1} + 2 \cdot Z_{SC}) \cdot \Delta I_{B1}]} \quad (18)$$

B. Compensation at the Middle of TL:

To obtain fault location formula in the case of compensation at the middle of TL, the algorithm should be divided to two parts. The first part is for fault in front of the SC and the second algorithm for faults behind the SC.

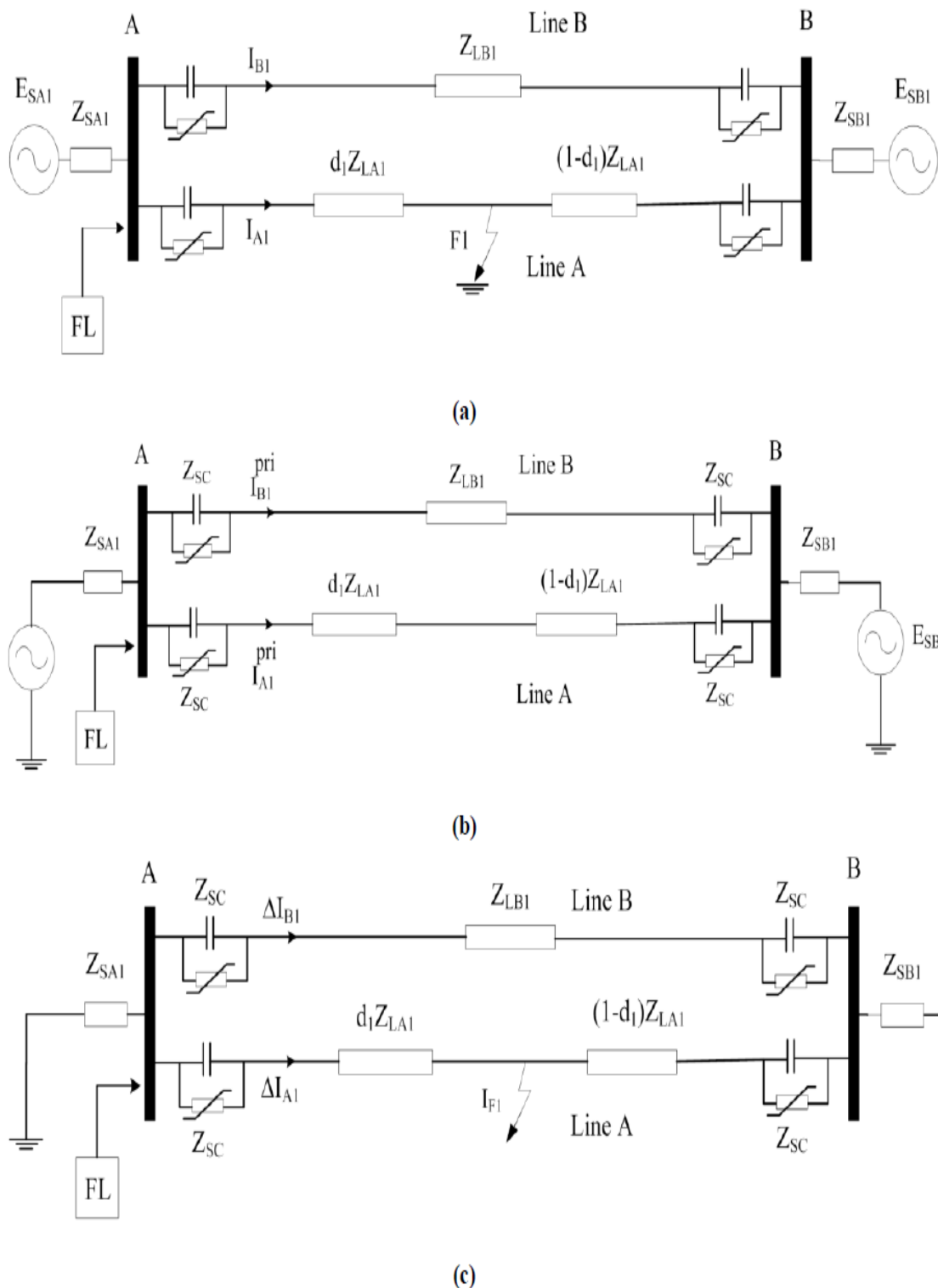


Fig. 6. A typical series compensated parallel TL with SC at the two ends, (a) positive sequence network after fault, (b) positive sequence network before fault, (c) superposition of positive sequence network.

Fig.7a illustrates the positive sequence network of a typical series compensated parallel TL which SC are located at middle of TL in which an arbitrary fault happened at F_2 between Bus A and SC.

Regarding to previous subsection, by applying the superposition principle to Figs. 7.a and 7.b, one can conclude the Fig. 7.c. Referring to Fig. 7.c, for a fault occurring at an arbitrary distance d_2 from Bus A, by applying KVL in loop which includes the Line B, (19) obtained as below:

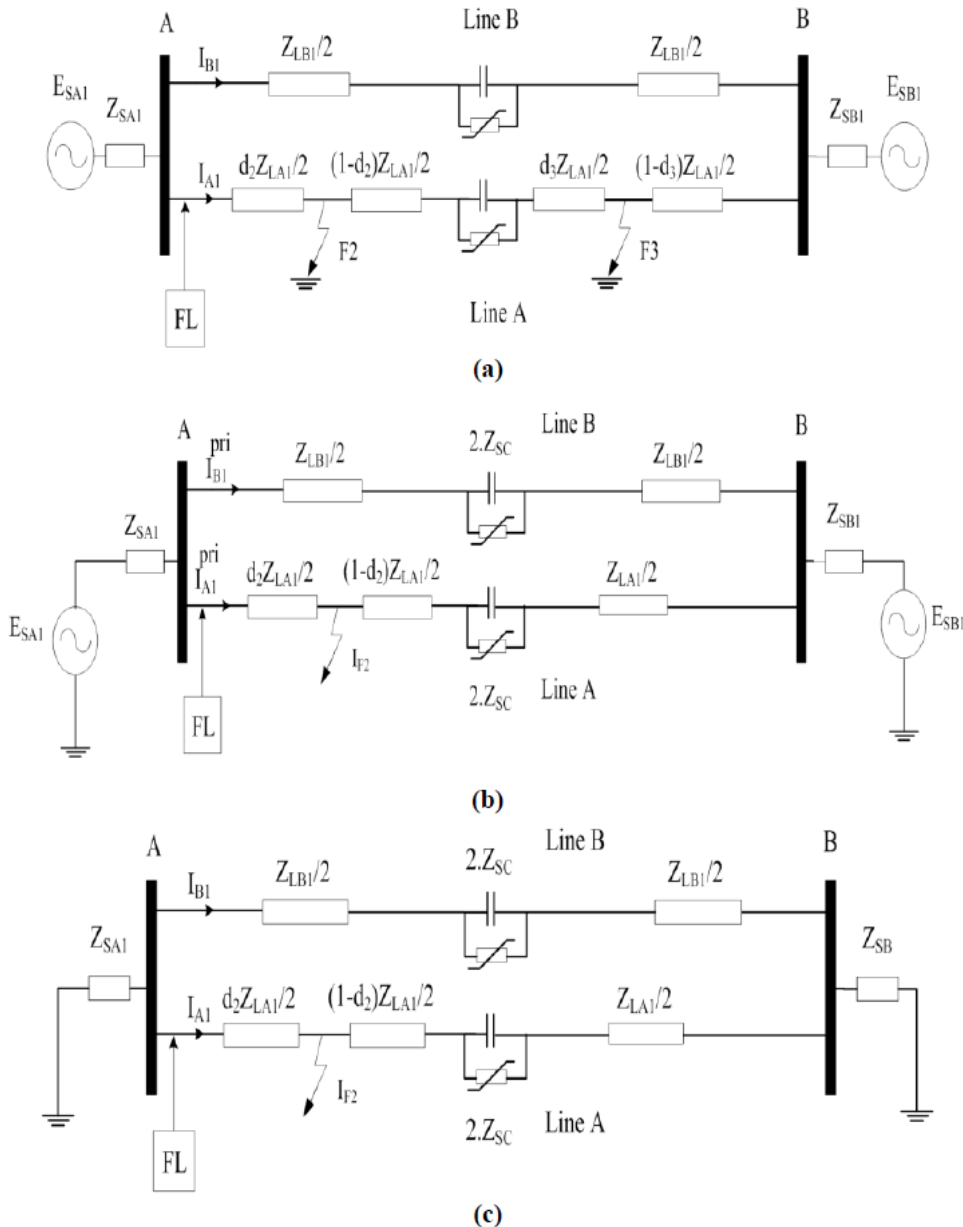


Fig. 7. A typical series compensated parallel TL with SC at the middle, (a) positive sequence network after fault, (b) positive sequence network before fault, (c) superposition of positive sequence network.

$$[2 \cdot Z_{SC} + Z_{LB1}] \cdot \Delta I_{B1} + \left[(1 - d_2) \cdot \frac{Z_{LA1}}{2} + 2 \cdot Z_{SC} \right] \cdot (I_{F2} - \Delta I_{A1}) - \frac{d_2 \cdot Z_{LA1}}{2} \cdot \Delta I_{A1} = 0 \quad (19)$$

Similar to equation (19) and Referring to Fig. 7.c, by applying KVL in loop which includes the Line A, equation (20) obtained as below:

$$Z_{SA1} \cdot (\Delta I_{A1} + \Delta I_{B1}) + [2 \cdot Z_{SC} + Z_{LB1}] \cdot \Delta I_{B1} + Z_{SB1} \cdot (\Delta I_{A1} + \Delta I_{B1} - I_{F2}) = 0 \quad (20)$$

Elimination of I_{F2} from the (19) and (20) yields the following formula for a sought distance to fault:

$$d_2 = \frac{2 \cdot Z_{SA1} + 4 \cdot Z_{SC}}{Z_{LA1}} \quad (21)$$

$$2. \frac{Z_{SB1} \cdot \left[\frac{Z_{LA1}}{2} \Delta I_{A1} + (Z_{LA1} + 2 \cdot Z_{SC}) \cdot \Delta I_{B1} \right]}{Z_{LA1} \cdot [(Z_{SA1} + Z_{SB1}) \cdot (\Delta I_{A1} + \Delta I_{B1}) + (Z_{LB1} + 2 \cdot Z_{SC}) \cdot \Delta I_{B1}]}$$

Regarding to previous figures, by applying the superposition principle to Figs. 7.a and 7.b for a fault behind the SC, one can conclude the Fig.8. Referring to Fig.8, for a fault occurring at an arbitrary distance d_3 from Bus A, by applying KVL in loop which includes the Line B, equation (22) obtained as below:

$$\begin{aligned} [2 \cdot Z_{SC} + Z_{LB1}] \cdot \Delta I_{B1} + \left[(1 - d_3) \cdot \frac{Z_{LA1}}{2} \right] \cdot (I_{F3} - \Delta I_{A1}) - \left[\frac{(d_3 + 1) \cdot Z_{LA1}}{2} + 2 \cdot Z_{SC} \right] \cdot \Delta I_{A1} = 0 \end{aligned} \quad (22)$$

Similar to equation (22) and Referring to Fig.8, by applying KVL in loop which includes the Line A, equation (23) obtained as below:

$$\begin{aligned} Z_{SA1} \cdot (\Delta I_{A1} + \Delta I_{B1}) + [2 \cdot Z_{SC} + Z_{LB1}] \cdot \Delta I_{B1} + Z_{SB1} \cdot (\Delta I_{A1} + \Delta I_{B1} - I_{F3}) = 0 \end{aligned} \quad (23)$$

Elimination of I_{F3} from the equations (22 and 23) yields the following formula for a sought distance to fault:

$$d_3 = 1 - 2 \cdot \frac{Z_{SB1} \cdot [(Z_{LA1} + 2 \cdot Z_{SC}) \Delta I_{A1} - (Z_{LB1} + 2 \cdot Z_{SC}) \cdot \Delta I_{B1}]}{Z_{LA1} \cdot [(Z_{SA1} + Z_{SB1}) \cdot (\Delta I_{A1} + \Delta I_{B1}) + (Z_{LB1} + 2 \cdot Z_{SC}) \cdot \Delta I_{B1}]} \quad (24)$$

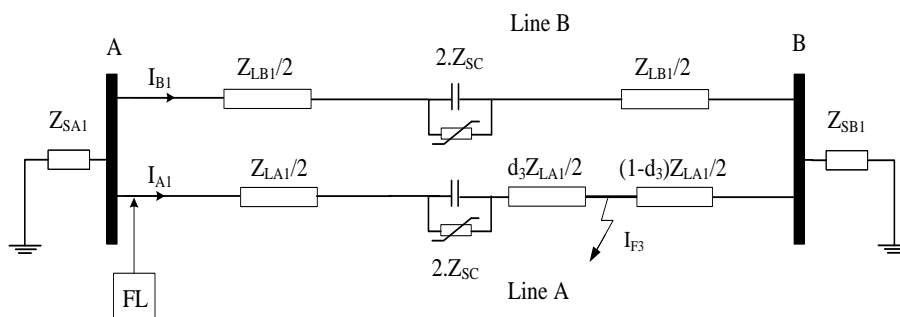


Fig. 8. A typical series compensated parallel TL with SC at the middle, superposition of positive sequence network for faults behind the SC.

IV. SIMULATION RESULT

This section describes the results acquired using the proposed algorithm and its performance when it is subjected to different tests.

A. Simulated Model:

The details of the system simulated are as follows. The 50 Hz, 400 kV power system transmitting 3000 MVA from a power plant to an equivalent load system through a 300 km TL which compensated with SC. The series compensated parallel TL with 300 km length and 70% compensation by SC is considered for this study. Series compensation is done on TLs to increase the transmission capability of the system. In general cases, for series compensation at the middle of the TL and compensation at the two ends, one SC bank with $C=25 \mu\text{F}$ and two SC bank with $C= 50 \mu\text{F}$ is considered, respectively.

Moreover, the system is compensated and studied for different compensation levels to study the effect of compensation level. Series capacitor banks on both the lines are similar. The TL inductance, capacitance and resistance considered are $L= 1.369 \text{ mH/km}$, $C= 8.49\text{nF/km}$, $R= 5.63 \text{ m}\Omega/\text{km}$.

To obtain accurate results, the distributed model of TLs is used in the simulations. The TLs prefault load flow is controlled by changing the phase angle of the sources at buses A and B. The initial value used for phase angles of the bus B is -15° with respect to the source at bus A, respectively.

B. Test Results:

In order to evaluate the proposed fault location algorithm many different fault cases have been studied. To consider all possibilities, each algorithm was investigated for all major types of faults for different fault pass resistance. Figs. 9 and 10 shows the per unit phase-to-ground voltage and current waveforms measured at bus A following an a-g fault with 1Ω fault resistance at 190 km away from fault locator at line A (Configuration of Fig.6a). The fault inception is at $t=0.2$ sec. Fig. 11 also shows the related distance to fault calculated by (18) which indicate the high accuracy of the proposed algorithm.

Fig. 12 also shows the fault location result for a single-phase-to-ground fault following a b-g fault with 10Ω fault resistance at 70 km away from fault locator at line A (Configuration of Fig. 7.a). As we can see from the figure, transients of the output signal die out rapidly and the final value for fault locator can be accessible only after 100 msec which indicates the speed of the algorithm.

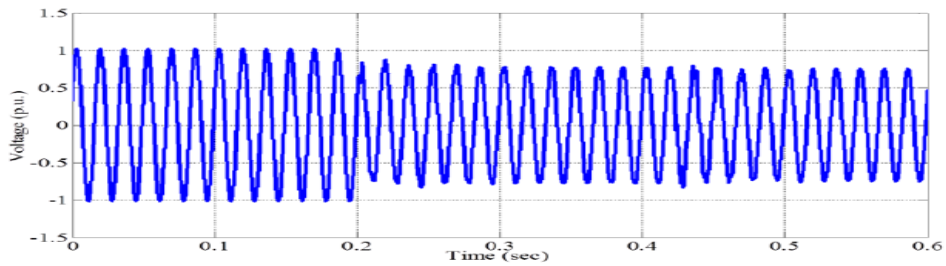


Fig. 9. Per unit voltage signal of Bus A before and during an a-g fault at 190km from Bus A.

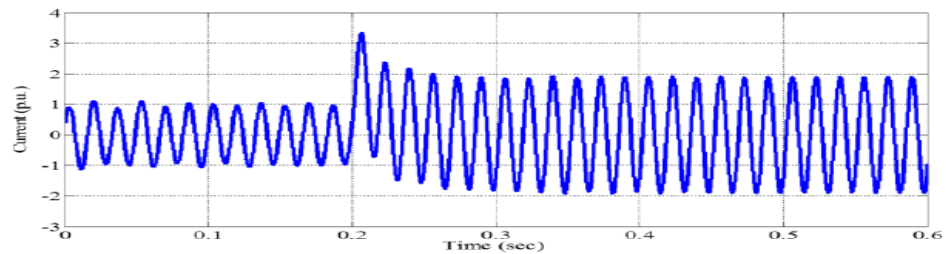


Fig. 10. Per unit current signal of Bus A before and during an a-g fault at 190km from Bus A.

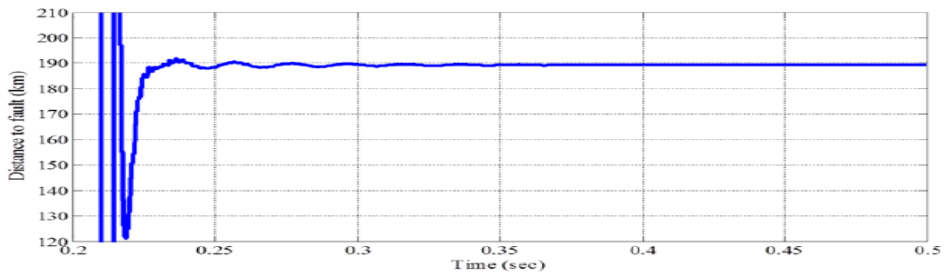


Fig. 11. Output of equation (18) for an a-g fault at 190km from Bus A.

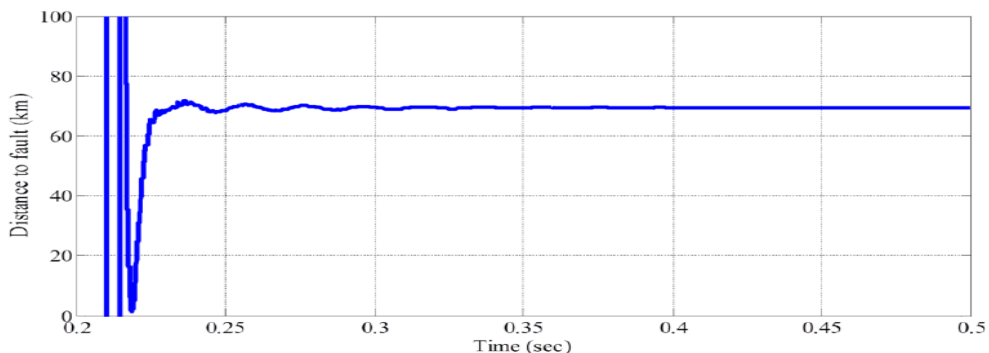


Fig. 12. Output of equation (21) for a b-g fault at 70km from Bus A.

For more examination, the algorithm is tested for various fault location with different fault resistance. Figs. 13 and 14 are the results for the series compensation configuration which is indicated in Fig. 6.a and Fig. 7.a, respectively. According to Fig. 13, the error in calculation of the fault distance increases when the fault point reaches to far end terminal. On the other hand, the error will increase with the increase of fault resistance. Moreover, from Fig. 13, one can conclude that the effect of fault resistance on fault location algorithm error increases when the fault occurs nearby the far end terminal because of infeed current from the far end terminal.

All have been concluded above are true for Fig. 14 besides the effect of series compensation at the middle of the TL. It causes a jump in error value after the SC which locates at 150 km of Bus A. In the worst case, if a single-phase-to-ground fault with 100 Ω resistance occurs nearby the far end terminal (configuration of Fig. 6.a), the error is just around 1.8 %. Comparing the algorithm results to previous works, one can conclude that the algorithm presents accurate and acceptable result even in the case of borderline high resistance faults. However, most of the authors fail to report the results of their algorithms for borderline and high resistance faults.

However the above test cases are for 70% compensation, it is necessary that the algorithm be examined for different compensation ratio. To fulfill that, we considered different level of compensation from zero to 70 percent. Then a bc-g fault at 250 km from bus A is applied to the network in both configurations mentioned before. Fig. 15 shows the error of fault location algorithm which is calculated by (18) for three values of fault resistance. Fig. 16 also shows the same error which is calculated by (21). In both cases the error of calculation increases by increase of compensation level. By investigating these figures, one can deduce that the effect of fault resistance is more sensible when the compensation level is low.

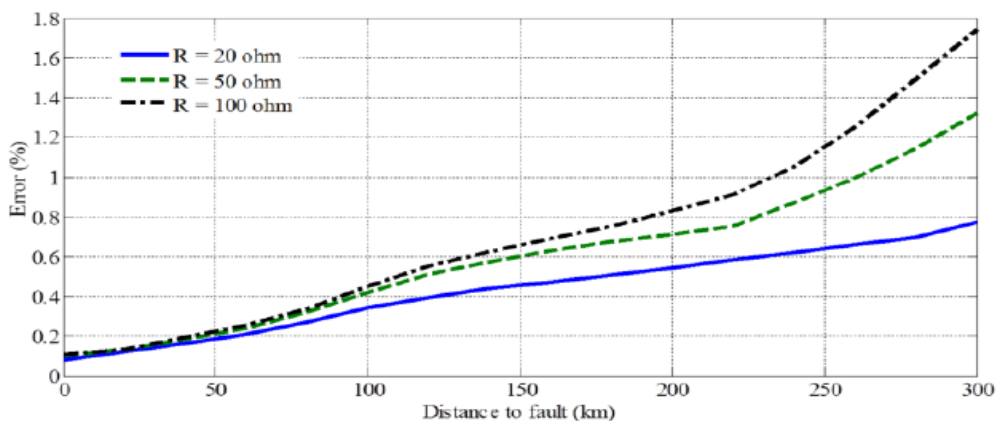


Fig. 13. Single-phase-to-ground fault through line A with compensation at two ends of TL.

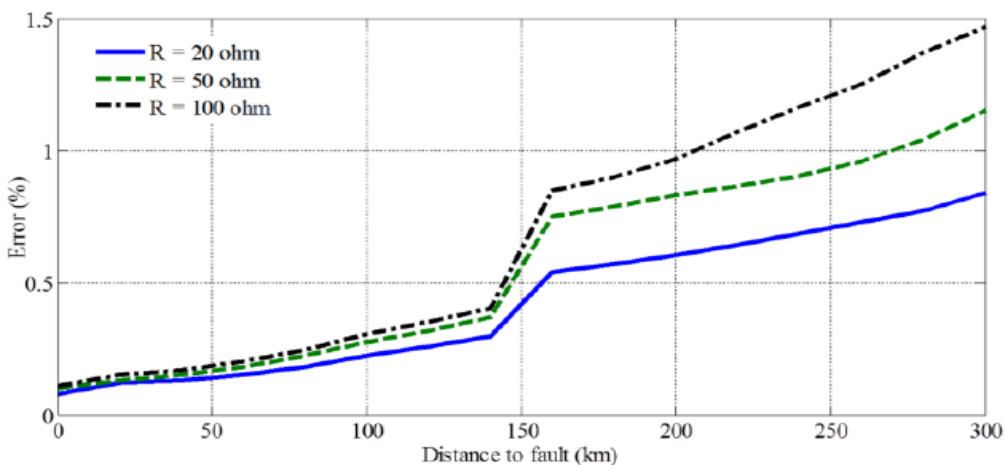


Fig. 14. Single-phase-to-ground fault through line A with compensation at the middle of TL

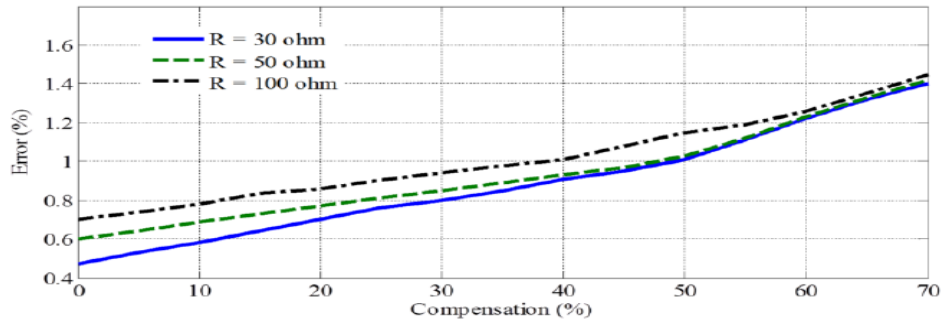


Fig. 15. Effect of compensation level on fault location algorithm (configuration of Fig. 6.a)

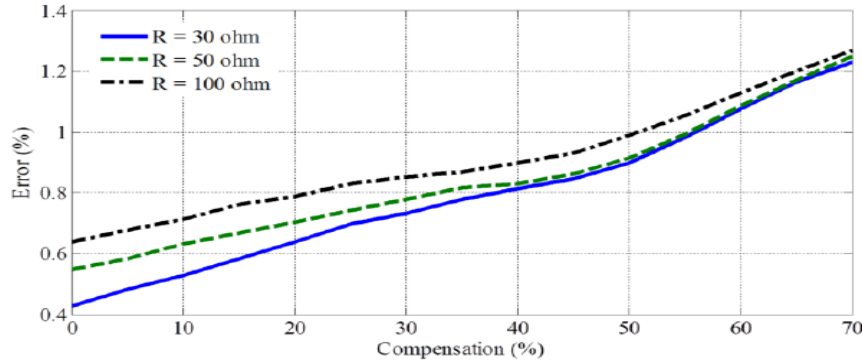


Fig. 16. Effect of compensation level on fault location algorithm (configuration of Fig. 7.a)

Tables I and II are also show the supplimentary tests condition and related fault location errors for configuration indicated in Fig. 6.a and Fig. 7.a, respectively. Different fault inception angles and fault distance from bus A are considered. The results indicate that in the worst case the fault location error is not exceed 0.8 %. From these tables one can conclude that the fault inception angle has no effect on the proposed fault location algorithm.

Table I

Fault Distance Estimation With Regard To Changing The Fault Distance And Fault Inception Angle For Configuration Fig.6a

Distance to Fault (p.u.)	Fault inception angle (°)	Measured error (%)
0.05	30	0.07
0.1	45	0.11
0.2	0	0.12
0.3	60	0.17
0.4	120	0.22
0.5	135	0.27
0.6	150	0.34
0.7	90	0.41
0.8	180	0.49
0.9	15	0.6
0.95	75	0.78

Table II

Fault Distance Estimation With Regard To Changing The Fault Distance And Fault Inception Angle For Configuration Fig.7a

Distance to Fault (p.u.)	Fault inception angle (°)	Measured error (%)
0.05	30	0.06
0.1	45	0.16
0.2	0	0.21
0.3	60	0.27
0.4	120	0.4
0.5	135	1.18
0.6	150	0.41
0.7	90	0.32
0.8	180	0.33
0.9	15	0.37
0.95	75	0.48

V. CONCLUSION

A new fault location algorithm for series compensated parallel TLs was presented in this paper which just utilizes the information of the local end of the transmission lines. The advantage of the algorithm can be classified in below items:

- 1) The proposed algorithm does not require current or voltage signals from the far end terminal which is frequently does not have proper communicational channel to send synchronized data.
- 2) This algorithm does not use the voltage signals at all, so it works independent of the effect of voltage transformer transient problem like ferroresonance phenomena.
- 3) Test results demonstrate high accuracy even in the case of boundary faults.
- 4) It covers all fault types and no limit is considered for the magnitude of fault resistance.

Furthermore, Basic principles and detail formulation are illustrated and variety of the test condition also verifies that how the algorithm is precise and robust. Effect of different condition such as compensation level, fault impedance, fault inception angle and location of fault are studied and reported. High accuracy of the algorithm in these cases distinguishes it as a proper way of locating fault in series compensated parallel TLs.

REFERENCES

- [1] A. A. Girgis, "A new Kalman filtering based digital distance relay," IEEE Trans. Power App. Syst., vol. PAS-101, no. 9, pp. 3471-3480, Sep. 1982.
- [2] A. Esmailian, et al. "Distance Protection Algorithm for Three Terminal Transmission Lines Using Local Measurements," International Journal of Review on Modelling and Simulations, Vol. 5, No. 6, Oct. 2012.
- [3] E. M. Pereira and L. C. Zanetta, "Fault Location in Transmission Lines Using One-Terminal Post-fault Voltage Data," IEEE Transactions on Power Delivery, Vol. 19, No. 2, pp. 570-575, Apr. 2004.
- [4] T. Kawady, J. Stenzel, "A practical fault location approach for double circuit transmission lines using single end data," IEEE Transactions on Power Delivery, Vol. 18, No. 4, pp. 1166-1173, Oct. 2003.
- [5] M. Farshad, J. Sadeh, "Accurate Single-Phase Fault-Location Method for Transmission Lines Based on K-Nearest Neighbor Algorithm Using One-End Voltage," IEEE Transactions on Power Delivery, Vol. 27, No. 4, pp. 2360-2367, Oct. 2012.
- [6] A. Esmailian, et al. "A Novel Fault Location Algorithm for Multi-Tapped Transmission Lines Using Local Measurement", International Journal of Review on Modeling and Simulations, Vol. 4, No. 5, Oct. 2011.
- [7] H. Ha, B. H. Zhang, Z. L. Lv, "A Novel Principle of Single-Ended Fault Location Technique for EHV Transmission Lines," IEEE Transactions on Power Delivery, Vol. 18, No. 4, pp. 1147-1151, Oct. 2003.
- [8] Z. Qingchao, et. al, "Fault Location of Two-parallel Transmission Line for Non-earth Fault Using One-terminal Data," IEEE Transactions on Power Delivery, Vol. 14, No. 3, pp. 863-867, Jul. 1999.
- [9] A. Esmailian, M. Kezunovic, "An Impedance Based Fault Location Algorithm for Tapped Lines Using Local Measurements," The 45th North American Power Symposium (NAPS2013), Manhattan, KS, USA, September 2013.
- [10] Y. Liao and S. Elangovan, "Unsynchronized two-terminal transmission-line fault-location without using line parameters," IEE Proc.-Gener. Transm. Distrib. Vol. 153, No. 6, pp. 639-643, Nov. 2006.
- [11] M. Kezunovic, B. Perunicic, "Automated Transmission Line Fault Analysis Using Synchronized Sampling at Two Ends," IEEE Transactions on Power Systems, Vol. 11, No. 1, February 1996.
- [12] A. Esmailian, T. Popovic, M. Kezunovic, "Transmission Line Relay Mis-operation Detection Based on Time-Synchronized Field Data," Electric Power Systems Research Journal, Vol. 125, pp.174-183, 2015.
- [13] J. Izykowski, et. al, "Accurate Noniterative Fault Location Algorithm Utilizing Two-End Unsynchronized Measurements," IEEE Transactions on Power Delivery, Vol. 25, No. 1, pp. 72-80, Jan. 2010.
- [14] E. G. Silveira and C. Pereira, "Transmission Line Fault Location Using Two-Terminal Data Without Time Synchronization," IEEE Transactions on Power Delivery, Vol. 22, No. 1, pp. 498-499, Feb. 2007.

- [15] P. Dutta, A. Esmailian, M. Kezunovic, "Transmission-Line Fault Analysis Using Synchronized Sampling," IEEE Trans. Power Delivery, Vol. 29, No. 2, April 2014.
- [16] E. G. Silveira and C. Pereira, "Transmission Line Fault Location Using Two-Terminal Data Without Time Synchronization," IEEE Transactions on Power Delivery, Vol. 22, No. 1, pp. 498-499, Feb. 2007.
- [17] A. Esmailian, M. Mohseninezhad, M. Khanabadi, M. Doostizadeh, "A Precise PMU Based Fault Location Method for Multi Terminal Transmission Line Using Voltage and Current Measurement", 10th International Conference on Environment and Electrical Engineering, pp. 536-540, 8-11 May 2011.
- [18] L. B. Sheng and S. Elangovan, "A fault location method for parallel transmission lines," Int. J. Elect. Power Energy Syst. vol. 21, no. 4, pp. 253-259, May 1999.
- [19] T. Kawady and J. Stenzel, "A practical fault location approach for double circuit transmission lines using single end data," IEEE Trans. Power Del., vol. 18, no. 4, pp. 1166-1173, Oct. 2003.
- [20] G. Song, J. Suonan, and Y. Ge, "An accurate fault location algorithm for parallel transmission lines using one-terminal data," Elect. Power Energy Syst., vol. 31, no. 2-3, pp. 124-129, Mar. 2009.
- [21] J. Suonan, G. Song, Q. Xu, and Q. Chao, "Time-domain fault location for parallel transmission lines using unsynchronized currents," Elect. Power Energy Syst., vol. 28, no. 4, pp. 253-260, May 2006.
- [22] Novosel, D. G. Hart, E. Udren, and J. Garitty, "Unsynchronized two-terminal fault location estimation," IEEE Trans. Power Del., vol. 11, no. 1, pp. 130-138, Jan. 1996.
- [23] J. Izykowski, R. Molag, E. Rosolowski, and M. Saha, "Accurate location of faults on power transmission lines with use of two-end unsynchronized measurements," IEEE Trans. Power Del., vol. 21, no. 2, pp. 627-633, Apr. 2006.
- [24] J. Izykowski, E. Rosolowski, P. Balcerek, M. Fulczyk, and M. M. Saha, "Accurate non-iterative fault location algorithm utilizing two-end unsynchronized measurements," IEEE Trans. Power Del., vol. 25, no. 1, pp. 72-80, Jan. 2010.
- [25] M. M. Saha, J. Izykowski, E. Rosolowski, and B. Kasztenny, "A new accurate fault locating algorithm for series compensated lines," IEEE Trans. Power Del., vol. 14, no. 3, pp. 789-797, Jul. 1999.
- [26] J. Sadeh, N. Hadjsaid, A. M. Ranjbar, and R. Feuillet, "Accurate fault location algorithm for series compensated transmission lines," IEEE Trans. Power Del., vol. 15, no. 3, pp. 1027-1033, Jul. 2000.
- [27] E. Mohagheghi, et. al, "A New Fault Location Method Based on Adaptive Neuro Fuzzy in Presence of SSSC on Transmission Line", 11th International Conference on Environment and Electrical Engineering, pp. 108-111, 18-25 May 2012.
- [28] Novosel, B. Bachmann, D. Hart, Y. Hu, and M. M. Saha, "Algorithms for locating faults on series compensated lines using neural network and deterministic methods," IEEE Trans. Power Del., vol. 11, no. 4, pp. 1728-1736, Oct. 1996.
- [29] M. M. Saha, K. Wikstrom, J. Izykowski, and E. Rosolowski, "Fault location in uncompensated and series-compensated parallel lines," in Proc. IEEE Power Eng. Soc. Winter Meeting, Singapore, Jan. 2000, vol. 6, pp. 23-27, CD-ROM.
- [30] Y. Evrenosoglu and A. Abur, "Fault location for teed circuits with mutually coupled lines and series capacitors," presented at the IEEE Bologna Power Tech Conf., Bologna, Italy, 2003.
- [31] L. Goldworthy, "A Linearized Model for MOV-Protected Series Capacitors," IEEE Trans. on Power Systems, Vol. 2, No. 4, pp. 953-958, Nov. 1987.